Thermal Fatigue of Austenitic Stainless Steel : Influence of Surface Conditions

A.Le Pécheur[a,b], M.Clavel[a], F.Curtit[b] , C.Rey[a], J.M.Stephan[b], Ph.Bompard[a]

[a]Laboratoire MSSMat, UMR 8579 CNRS, Ecole Centrale Paris, Grande voie des Vignes, 92295 Châtenay-Malabry Cedex France
[b] Département MMC, EDF R&D, Site des Renardières, Route de Sens Ecuelles, 77250 Moret-sur-Loing, France

Abstract A thermal fatigue test (INTHERPOL) was developed by EDF in order to study the initiation of cracks. These tests are carried out on tubular specimens under various loadings, surface finish qualities and welding in order to give an account of these parameters on crack initiation. The main topic of this study is the research of a fatigue criterion using a micro/macro modelling approach.

1 INRODUCTION

Some cases of cracking of 304L austenitic stainless steel components due to thermal fatigue were encountered in particular on the Residual heat removal circuits (RHR) of the pressurized water reactors (PWR). EDF has initiated a R&D program to understand and assess the risks of damage on nuclear plant mixing zones. The INTHERPOL test developed at EDF R&D is designed in order to perform pure thermal fatigue test on tubular specimen under mono-frequential thermal load. The first part of work deals with material characterization (stainless steel 304L) emphasing the specificities of the surface roughness link with a strong hardening gradient. Micro hardness measurements and TEM observations were intensively used to characterize this gradient. The second part is the macroscopic modelling of INTHERPOL tests in order to determine the components of the stress and strain tensors due to thermal cycling. The third part of work is thus to evaluate the effect of surface roughness and hardening gradient using a calculation on a finer scale. This simulation is based on the variation of dislocation density. A goal for the future is the determination of the fatigue criterion mainly based on polycrystalline modelling. Stocked energy or critical plane being available that allows making a sound choice for the criteria.

2 INTHERPOL THERMAL FATIGUE TEST

INTHERPOL thermal fatigue tests are carried out on tubular specimens in austenitic stainless steel 304L. The INTHERPOL facility is designed to apply thermal cycles controlled in frequency and amplitude (Curtit, 2005). The specimens consist of a 300 mm length section of pipe with an internal diameter of 386mm and a thickness of 10mm. Thermal cycling is applied to a 70mm broad sector of internal surface. The cold part of the cycle is obtained by pulverization of a water spray on hot surface and the heating is obtained by infra red radiation. During the test the specimen is moved with an alternated rotation in order to expose the test sector alternatively to the spray and to the infrared radiation as shown in figure 1. Five tests have been carried out with a thermal amplitude of 120° to 140°C and a cycle's duration ranging of 5 to 8 seconds, including several surface finish. During the test, the temperature is measured by using thermocouples. The recorder temperature as used as input data to perform finite element simulations in order to obtain the stress and strain fields to interpret experimental results. The whole experimental result shows a significant effect of the surface finishing on fatigue damage sensitivity.

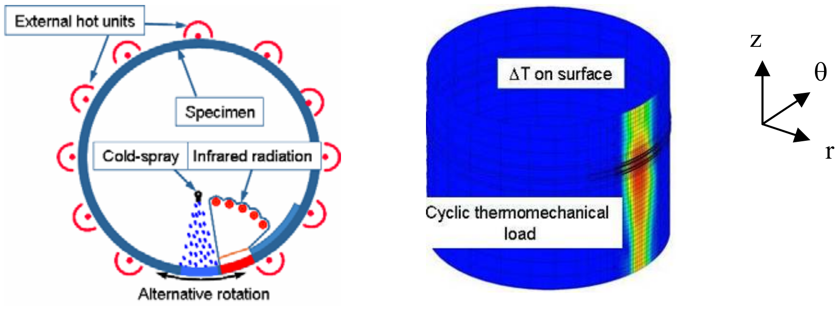

Figure 1. INTHERPOL thermal fatigue test.

3 MATERIAL CHARACTERIZATION (AUSTENITIC STAINLESS STEEL 304L)

3.1 Work-hardening gradient

According to the test considered, the specimens have various industrial surface finishes. On this study, the first INTHERPOL test with raw surface finish is observed. The first results of the characterization on the surface show a strong work-hardening gradient located on a 250 microns layer due to the surface machining (Figure 2). Micro hardness testing and TEM observations (Table 1) show this work hardening gradient, in agreement with previous results (Petitjean, 2003). The initial dislocation density in the material is $9.10^{12}m^{-2}$. Beneath this surface the dislocation density reach 10^{14} m^{-2} at about 300µm (Figure 3(a)). Furthermore extended staking faults are also observed. Twinning takes place at 200µm with an increasing density to the surface (Figure 3(b)). It must also be noticed the occurrence of a transformed zone (looking like a recristallisation zone) $\gamma \rightarrow \alpha$' (bcc) (Figure 3(c)).

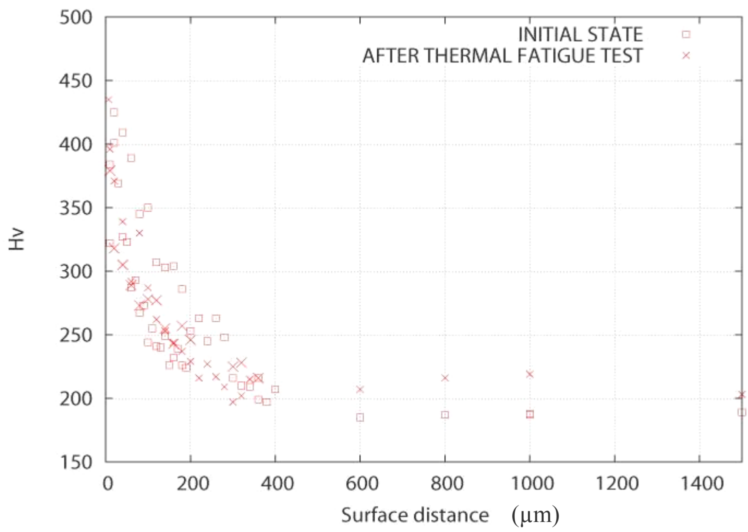

Figure 2 : work -hardening gradient on a 250 microns layer – Hardness measurements

Table I. Work-hardening gradient

Surface distance (µm)	TEM Observations	Microhardness Measurements (Hv)
Core	Low dislocation density	180
300	High dislocation density	200
250	Extended stacking faults and high dislocations density	225
200	Beginning of twinning	250
150	Numerous twins	275
2	High twins density and recrystallisation zone	> 400

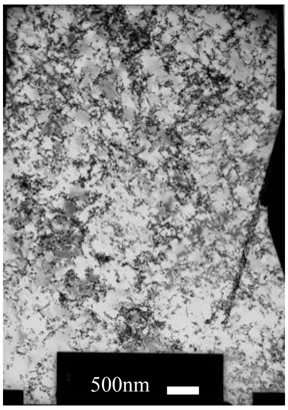

(a) High dislocation density
d = 300µm

(b) Twinning
d = 200 µm

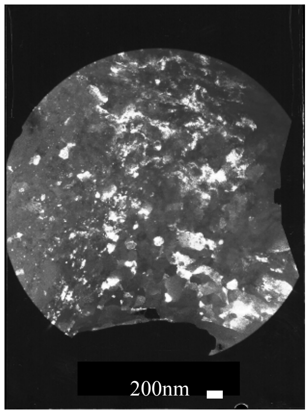

(c) transformation Zone (bcc nanograins) d = 2 µm

Figure 3. TEM Observations.

3.2 Roughness and residual stresses

Residual stresses measurements on surface in axial and circumferential directions were done (Lebrun, 2003) on INTHERPOL tubular models. The initial residual stresses are 200 MPa in the axial direction and 400 MPa in the circumferential one. These stresses decrease during thermal fatigue and reach -200 MPa for the axial direction and -400 MPa for the circumferential direction. Cartographies of the surface relief exhibit a strong average roughness with a lot of cuttings by stock removal and surface machining stries reach 50µm depth (about one grain size).

4 MACROCROSCOPIC MODELLING

As described in the experimental part, the internal surfaces of INTHERPOL specimens are instrumented with thermocouples. Consequently, the strain and stress state of the specimen during thermal cycling is only available by numerical simulation. Tests is simulated with the finite element code Code_Aster developed by EDF. The first step of the calculation is a thermo-elastic simulation of the test which will be used as input data for the mechanical simulation.

4.1 Behaviour law with memory effect

In order to determine the components of the stress and strain tensors due to thermal cycling, a mechanical calculation is realized. The surface characterization shows a work-hardening gradient on the first 250µm which does not evolved during thermal fatigue test. Then, the macroscopic modelling needs a pre-strain behaviour cyclic temperature law to capture the material behaviour on surface. An elastoviscoplastic law with an isotropic and two kinematics hardening has been chosen (Nouailhas, 1988). The memory effect is introduced with a new hardening variable defining a new yielding surface in the strain space.

$$f\left(\underline{\underline{\varepsilon}}^{P}\right)=\frac{2}{3}J_{2}\left(\underline{\underline{\varepsilon}}^{P}-\underline{\underline{\zeta}}\right)-q=0 \qquad (1)$$

Recovery is not taken into account to reduce the number of parameter of the law. Fourteen parameters at two temperatures must be identified.

4.2 Identification and first results

The law has been identified on tension-compression oligocyclic tests at room temperature and at 300°C with and without pre-hardening. A pre-hardening tensile test of 14% has been chosen to reproduce the properties of surface material. According to mechanical tests (hardness) and TEM observations (Changeux, 2001), this tensile pre-hardening represents the material properties located at about 150µm. Figure 4 shows the results of the identification at room temperature on oligocyclic tension-compression test at +/-0.3% with and without pre-hardening. Total strain is applied between +/-0.2% and +/-0.7% in the range of the INTHERPOL biaxial load.

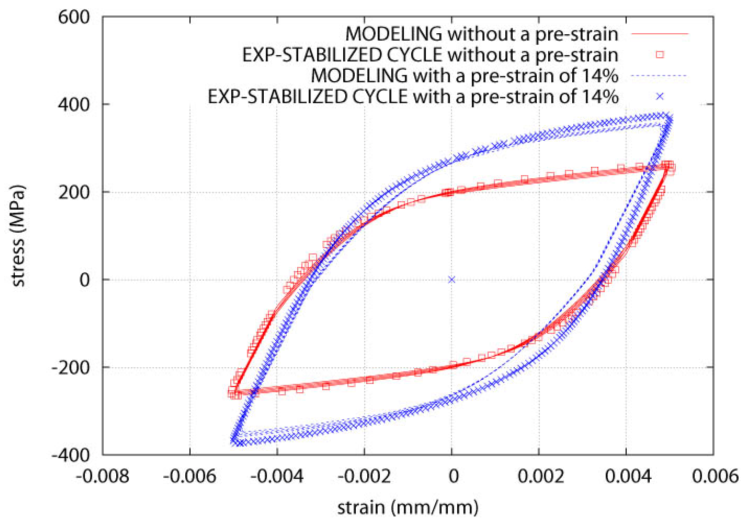

Figure 4. Identification of behaviour law with memory effect

A first modelling in Code_Aster without work-hardening and residual stresses gives a stabilized cycle of INTHERPOL loading after eight cycles. The thermo mechanical calculation is stabilized before the elastoviscoplastic mechanical calculation. It must be noticed that the loading path is essentially biaxial and non proportional (the phase lag reaches 30° in stress) as figure 5 shows.

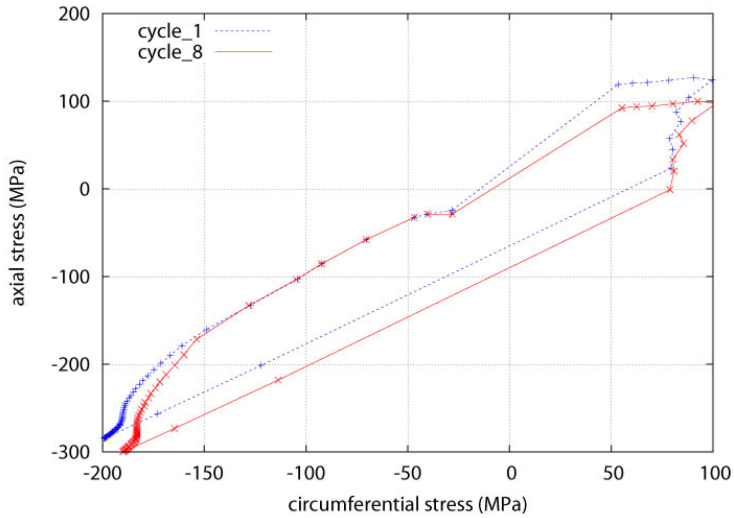

Figure 5. Loading path of INTHERPOL test

5 MESOSCOPIC MODELING

5.1 Crystal plasticity modeling

To take into account surface roughness and stress gradient at a finer scale, a mesoscopic approach was used (Erieau, 2004). The crytal plasticity model is able to capture the main characteristics of grain to grain heterogeneities, and obtained their formation and development with strain. In the lattest studies, validations with local and global measurements of deformation and rotation have been performed, and a good agreement between computation and experiments has been found. The model based on dislocation densities and accounts for crystallographic glide and lattice rotations. For f.c.c. systems, slip is considered to occur on the 12 {110}<111>

systems. The model is written in large deformation. On a slip system, plasticity is activated when the critical shear stress, τ_c^s, define with the Schmid criteria, is reached:

$$\left|\tau^s - x^s\right| = \tau_c^s \quad \text{and} \quad \left|\dot{\tau}^s - \dot{x}^s\right| = \dot{\tau}_c^s \tag{2}$$

The glide velocity is expressed with a classical viscoplastic potential based on the resolved shear stress and the critical shear stress for glide activating on system (s). A kinematic hardening x^s is introduced to take into account the cyclic behaviour of 304L (Baushinger effect) :

$$\dot{\gamma}_s = \dot{\gamma}_0 \left(\frac{\left|\tau^s - x^s\right|}{\tau_c^s} \right)^n \quad \text{if } \left|\tau^s - x^s\right| > \tau_c^s \qquad \dot{\gamma}_s = 0 \ \text{otherwise} \tag{3}$$

$\dot{\gamma}_0{}^s$ is a reference shear rate and n is a rate exponent. On a particular slip system, the dislocation density $\dot{\rho}^s$ evolution is governed by a production term based on Orowan's relationship and is balanced by annihilation term which takes into account the dynamic recovery during deformation.

$$\dot{\rho}_s = \frac{\dot{\gamma}_s}{b}\left[\frac{1}{L^s} - g_c \rho_c\right] \tag{4}$$

g_c is a parameter to an annihilation distance of dislocation. L^s is the average mean free path of the dislocations on the system (s), which is the material grain size at the onset of plastic deformation. A local hardening law (forest hardening) is introduced and gives the critical stress related to the dislocations density :

$$\tau_c^s = \tau_0 + \mu b \sqrt{\sum_u a_{su} \rho^u} \tag{5}$$

μ is the isotropic shear modulus, b the burger vector and τ_0 the friction stress. a^{su} is a hardening matrix whose terms depend on the type of elastic interactions between dislocation families (s) and (u). This matrix consists of six coefficients which could give a complete description of the hardening behaviour at small strains. Unfortunately, the identification of coefficients remains difficult to obtain (Franciosi,1984, Devincre, 2006).

5.2 Experimental procedure

A lot of previous studies have checked that good modelling necessitates a 3D crystallographic approach. The crystallographic orientations determination is carried out using a SEM and Orientation Imaging Microscopy (OIM) TSL analysis software. No particular texture is observed. Thus, the aggregate is realized with sixteen successive orientations cartography (Figure 6) and a finite element 3D mesh is created with ABAQUS®.

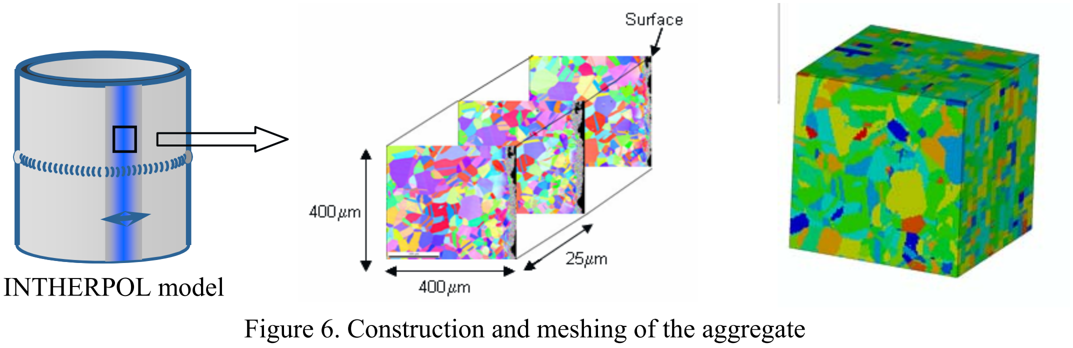

Figure 6. Construction and meshing of the aggregate

The crystal plasticity model has been implanted using a User Subroutine (UMAT). The numerical scheme is an explicit forward gradient procedure which gives a sufficient accuracy and a high integration speed.

5.3 Identification

Aggregate calculation is very huge and needs large memory, storage availability and a lot of time. For these reasons, the identification was done on stabilized parameters (microstructure observations and mechanical behaviour).

5.3.1 Mechanical results on Initial material (INTHERPOL core)

The initial material parameters are identified according to TEM observations and mechanical behaviour of oligocyclic fatigue tests. Then following initial parameters were available: dislocation density, mean free path of dislocations (cells size), isotropic and kinematic components (Figure 7) using the well known Cotrell's partition (Cottrell, 1953).

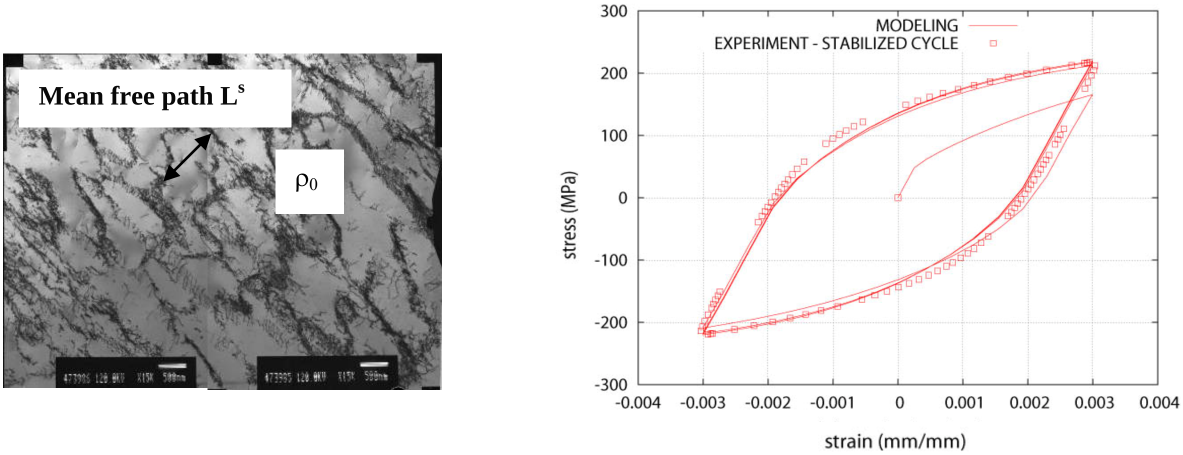

Figure 7 : TEM observations of tensile-compression test at +/- 0.3% at stabilized cycle. Comparison with simulation of the aggregate

5.3.2 Mechanical results at the surface material

A new identification is realized to reproduce the surface material. Some parameter have to be modified like the mean free path (grain size), the kinematic hardening and the yield stress. The figure 8 shows the results of oligocyclic fatigue test with the pre-hardening.

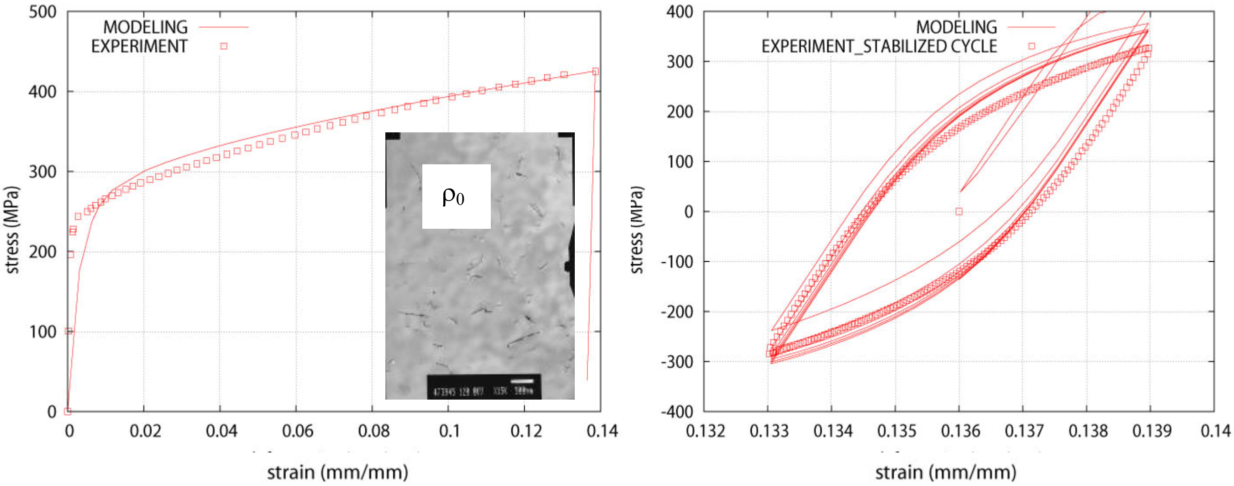

Figure 8 : TEM observations of initial material and tensile-compression test at +/- 0.3% at stabilized cycle . Comparaison with simulation of the aggregate for three deformation levels

6 CONCLUSION

At this time we have an aggregate model for cyclic loads identified for two materials: a core material a surface material. This model allows the evolution of various : dislocation density and energy, plastic work, elastic residual energy, strain and stress local fields…These variable can be determined , under INTHERPOL loading path, some localisation according to surface roughness, work-hardening gradient or crystalline orientations. As further works, three calculations will be done: a first with an initial material, a second with the work-hardening gradient and a third with the surface roughness. Using calculation, the main topic of this work being the determination of relevant macroscopic fatigue criteria.

7 REFERENCES

1. B.Changeux, Loi de comportement pour l'usinage-localisation de la déformation et aspects microstructuraux, PhD thesis, ENSAM-Angers, 2001.
2. AH.Cottrell, Dislocations and Plastic flow in crystals, *Oxford University Press*, London, 1953, 111-132.
3. F.Curtit and J.M.Stephan,, INTHERPOL Thermal Fatigue Test, *Pressure Vessels and Piping 2005*, Denver, July 17-21.
4. B.Devincre, L.Kubin and T.Hoc, Physical analysis of crystal plasticity by DD simulations, *Scripta Materiala*, 54, 2006, 741-746.
5. P.Erieau and C.Rey, Modeling of deformation, and rotation bands and of deformation induced grain boundaries in IF steel aggregate during large plane strain compression, *International Journal of plasticity*, 20, 2004, 1763-1788.
6. P.Franciosi, Etude théorique et expérimentale du comportement élastoplastique des monocristaux métalliques se déformant par glissement, PhD thesis, Paris-Nord university, France, 1984.
7. J.L.Lebrun, Rapport de mesures de contraintes résiduelles, ENSAM-Angers, 2003.
8. D.Nouailhas, Modélisation de l'écrouissage et de la restauration en viscoplasticité cyclique, *Revue de Physique appliqués*, 1988.
9. S.Petitjean, Influence de l'état de surface sur le comportement en fatigue à grand nombre de cycle de l'acier inoxydable austénitique 304L, PhD thesis, Poitiers University, France, 2003.